

Article

New Compounds with $[\text{As}_7]^{3-}$ Clusters: Synthesis and Crystal Structures of the Zintl Phases Cs_2NaAs_7 , $\text{Cs}_4\text{ZnAs}_{14}$ and $\text{Cs}_4\text{CdAs}_{14}$

Hua He, Chauntae Tyson and Svilen Bobev *

Department of Chemistry and Biochemistry, University of Delaware, Newark, Delaware 19716, USA;
E-Mails: nancyhe@udel.edu (H.H.); ctyson@udel.edu (C.T.)

* Author to whom correspondence should be addressed; E-Mail: bobev@udel.edu;
Tel.: +1-302-831-8720; Fax: +1-302-831-6335.

Received: 27 May 2011; in revised form: 16 June 2011/ Accepted: 21 June 2011 /

Published: 28 June 2011

Abstract: Three new cluster compounds, Cs_2NaAs_7 , $\text{Cs}_4\text{ZnAs}_{14}$, and $\text{Cs}_4\text{CdAs}_{14}$ were obtained from high temperature reactions. Their structures feature heptaarsenide $[\text{As}_7]^{3-}$ anions, where the clusters in $\text{Cs}_4\text{ZnAs}_{14}$ and $\text{Cs}_4\text{CdAs}_{14}$ are dimerized by the linkers Zn and Cd, respectively. The bonding characteristics of these clusters are discussed and compared. Band structure calculation on Cs_2NaAs_7 suggests that this compound is a semiconductor with an energy gap of *circa* 1.6 eV, which is in consistent with the dark red color of the crystals.

Keywords: cluster; arsenic; Zintl compound; crystal structure

1. Introduction

The typical Zintl phases are compounds formed between the alkali or alkaline-earth metals and the metalloids from group 13, 14, or 15 [1]. The chemical bonding in such systems could be rationalized following the Zintl-Klemm concept [2], which assumes that the electropositive elements act as electron donors (becoming spectator cations), while the electronegative counterparts form covalent bonds to obtain closed-shell electronic configurations. In recent years the field has been expanded to include some d-metals, as well as the nominally divalent Eu and Yb from the lanthanide family. Such materials, e.g., $\text{Yb}_{14}\text{MnSb}_{11}$ [3], $\text{Ca}_x\text{Yb}_{1-x}\text{Zn}_2\text{Sb}_2$ [4], and EuZn_2Sb_2 [5], among others, have received recognition for their potential in thermoelectric energy conversion [6]. There has also been a lasting research

interest in cluster-like Zintl ions [7], which is primarily instigated from the fundamental understanding of their bonding characteristics [7,8], as well as the novel properties offered by materials based on cluster assemblies [9-13].

In this article, we report three new Zintl compounds, Cs_2NaAs_7 , $\text{Cs}_4\text{ZnAs}_{14}$, and $\text{Cs}_4\text{CdAs}_{14}$, all of which feature the nortricyclane-like $[\text{As}_7]^{3-}$ clusters. In Cs_2NaAs_7 (formally $[\text{Cs}^+]_2[\text{Na}^+][\text{As}_7]^{3-}$) the $[\text{As}_7]^{3-}$ polyanions are discrete and “solvated” by Cs^+ and Na^+ cations, while $\text{Cs}_4\text{ZnAs}_{14}$, and $\text{Cs}_4\text{CdAs}_{14}$ (formally $[\text{Cs}^+]_4[\text{Zn}^{2+}]\{[\text{As}_7]^{3-}\}_2$ and $[\text{Cs}^+]_4[\text{Cd}^{2+}]\{[\text{As}_7]^{3-}\}_2$) are better viewed as containing larger heteroatomic $[\text{As}_7\text{-Zn-As}_7]^{4-}$ and $[\text{As}_7\text{-Cd-As}_7]^{4-}$ units, respectively. The latter can be considered as being made of two $[\text{As}_7]^{3-}$ species, bridged by tetrahedrally coordinated Zn and Cd atoms. The crystal structures and the bonding characteristics of the three compounds are presented, alongside with a discussion on the electronic structure of Cs_2NaAs_7 , calculated using the LMTO method [14-16].

2. Results and Discussion

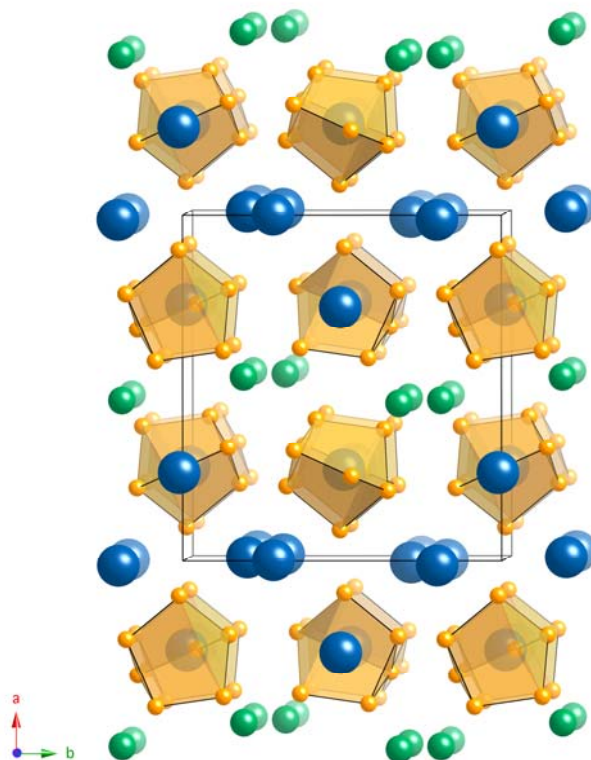
Cs_2NaAs_7 crystallizes in a monoclinic crystal system with space group $P2_1/c$ (No. 14, Pearson symbol $mP40$). Important crystallographic information pertaining to the structure is given in Table 1. Although it has identical formula to $A_3\text{As}_7$ ($A = \text{Li}, \text{Na}, \text{K}, \text{Rb}, \text{Cs}$) [17-19], it is not isostructural to any of the above-mentioned binary compounds. In Cs_2NaAs_7 , which is a true ternary phase, Cs and Na atoms are ordered on different crystallographic sites.

Table 1. Selected crystal data and structure refinement parameters for Cs_2NaAs_7 , $\text{Cs}_4\text{ZnAs}_{14}$, and $\text{Cs}_4\text{CdAs}_{14}$.

Empirical formula	Cs_2NaAs_7	$\text{Cs}_4\text{ZnAs}_{14}$	$\text{Cs}_4\text{CdAs}_{14}$
Formula weight	813.25	1645.89	1692.92
Space group, Z	$P2_1/c$, 4	$P2_1/c$, 16	$P2_1/c$, 4
Temperature		200(2) K	
Wavelength		Mo $K\alpha$, 0.71073 Å	
Cell parameters			
a (Å)	11.7671(18)	29.067(2)	10.608(3)
b (Å)	10.8528(17)	10.4714(8)	16.761(5)
c (Å)	10.2115(15)	43.039(3)	14.363(4)
β (°)	90.213(3)	128.0920(10)	91.785(5)
V (Å ³)	1304.1(3)	10309.9(14)	2552.6(12)
Calculated density (g/cm ³)	4.142	4.241	4.405
Absorption coefficient (cm ⁻¹)	231.94	243.43	244.74
Crystal size (mm ³)	0.044 × 0.030 × 0.028	0.068 × 0.049 × 0.023	0.080 × 0.060 × 0.040
Goodness-of-fit on F^2	1.001	0.979	0.981
R_1 ($I > 2\sigma$) ^a	0.0441	0.0436	0.0320
wR_2 ($I > 2\sigma$) ^a	0.0678	0.0737	0.0554
Largest diff. peak/hole (e ⁻ /Å ³)	1.172/-1.055	1.260/-1.463	1.012/-0.822
Weight coefficient, A/B ^a	0.0189/0	0/17.2682	0.0208/0

^a $R_1 = \sum ||F_o| - |F_c|| / \sum |F_o|$, $wR_2 = \{\sum [w(F_o^2 - F_c^2)^2] / \sum [w(F_o^2)^2]\}^{1/2}$, where $w = 1/[\sigma^2 F_o^2 + (AP)^2 + BP]$, and $P = (F_o^2 + 2F_c^2)/3$. A and B are weight coefficients.

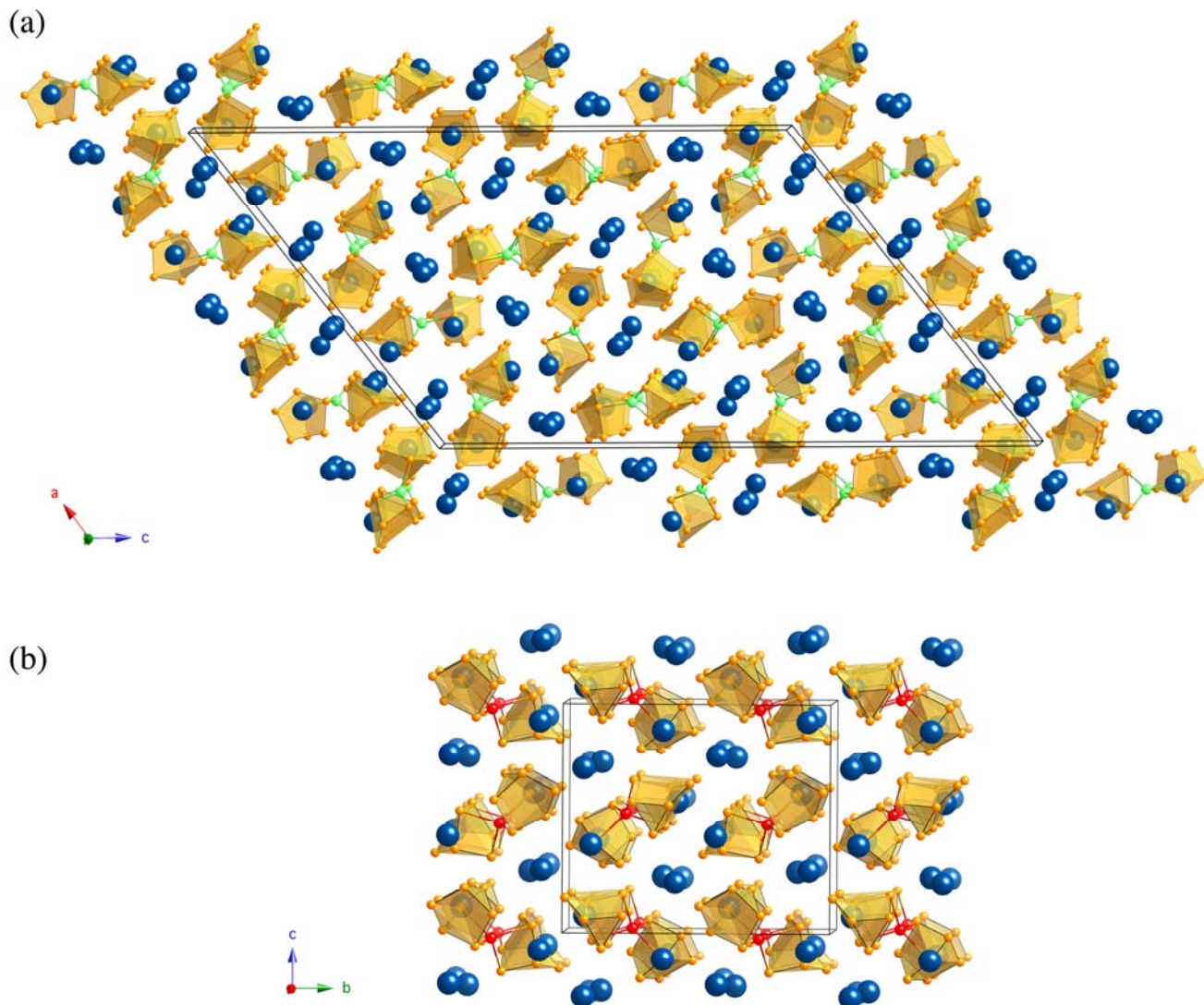
Figure 1. A schematic presentation of the crystal structure of Cs_2NaAs_7 . Color code: As—orange; Cs—dark blue; Na—green. The $[\text{As}_7]^{3-}$ clusters are depicted in polyhedral representation. The structure is projected approximately down the c -axis and the unit cell is outlined.



The packing of the $[\text{As}_7]^{3-}$ clusters resembles *fcc* arrangement with Cs^{2+} cations residing in the octahedral holes left between the clusters, and Cs^{1+} and Na^{+} cations in the tetrahedral holes, respectively (Figure 1). Such anion packing (*ABCABC*) is the same as in the structure of Cs_3As_7 [19], which is distinct from the double hexagonal close packing (*ABAC*) in K_3As_7 [19] and the hexagonal close packing (*ABAB*) in Rb_3As_7 [19].

$\text{Cs}_4\text{ZnAs}_{14}$ and $\text{Cs}_4\text{CdAs}_{14}$ also crystallize with the same monoclinic space group $P2_1/c$ (No. 14), but their structures are different (Table 1 and Figure 2). Notably, despite the same formulae, they are not isostructural to each other, with $\text{Cs}_4\text{ZnAs}_{14}$ having a four-times larger repeating unit (Pearson symbol *mP304*) than $\text{Cs}_4\text{CdAs}_{14}$ (Pearson symbol *mP76*). The detailed descriptions of each structure follow.

Figure 2. Schematic presentations of the crystal structures of (a) $\text{Cs}_4\text{ZnAs}_{14}$, and (b) $\text{Cs}_4\text{CdAs}_{14}$. Color codes: As—orange; Cs—blue; Zn—light green; Cd—red. The $[\text{As}_7]^{3-}$ clusters are depicted as translucent polyhedra, and the Zn–As and Cd–As bonds are highlighted. Unit cells and projection directions are outlined.



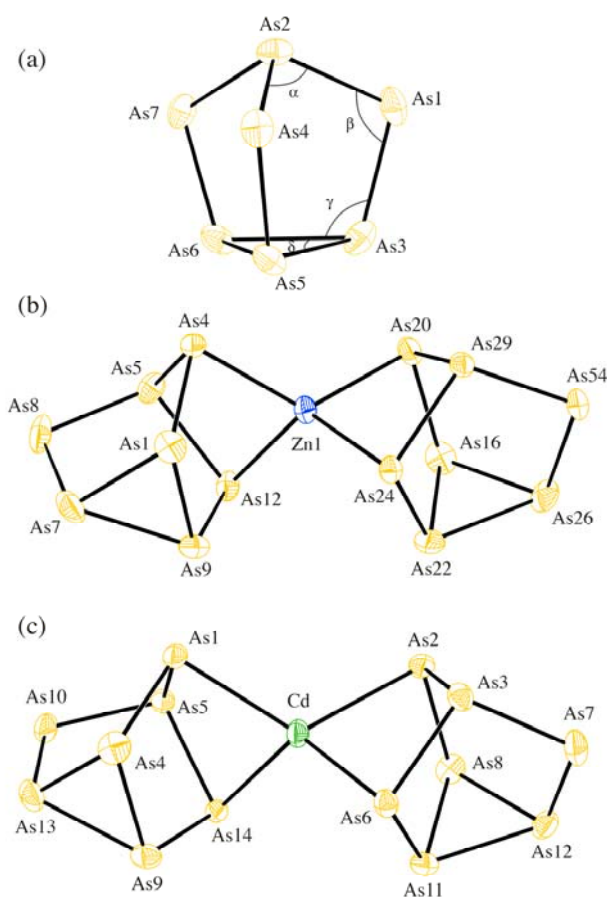
As already mentioned, the structure of Cs_2NaAs_7 features isolated nortricyclane-like (or birdcage-like) $[\text{As}_7]^{3-}$ clusters, with Cs^+ and Na^+ cations filling the space between them. The As–As distances (Table 2) could be grouped into three sets based on their length: set A, 2.4799(17)–2.5139(19) Å, which comprises the longest bonds, found between the As atoms of the triangular base (As3, As5, As6); the intermediate set B, which accounts for the bonds between the apical As (As2) and the three As atoms at the “waist” of the cluster (As1, As4, As7), ranging from 2.4042(18) to 2.4237(17) Å; and set C, which encompasses the shortest As–As contacts (2.3411(18)–2.348(2) Å), observed between the three basal As atoms and the three atoms in the waist (Figure 3(a)). Such distribution of bond distances seems to be a signature of all $[\text{As}_7]^{3-}$ cluster anions, as it is noted in the binary intermetallic compounds $A_3\text{As}_7$ ($A = \text{Li}, \text{Na}, \text{K}, \text{Rb}, \text{Cs}$) [17–19], as well as the compounds $[\text{Li}(\text{NH}_3)_4]_3\text{As}_7 \cdot \text{NH}_3$ [20], $[\text{Rb}(18\text{-crown-6})]_3\text{As}_7 \cdot 8\text{NH}_3$ [20], and $\text{Cs}_3\text{As}_7 \cdot 6\text{NH}_3$ [20], which are crystallized from liquid ammonia solutions. The bond angles are also characteristic, with α , β , γ , and δ (Figure 3(a)) close to 101° , 99° ,

105°, and 60°, respectively. These metric parameters are comparable with the corresponding angles in the above-mentioned compounds [17–20]. Following the Zintl-Klemm concept [2], the formal charges in the $[\text{As}_7]^{3-}$ clusters can be assigned as $(3b\text{-As}^0)_4(2b\text{-As}^-)_3$, and the Cs_2NaAs_7 formula can be readily rationalized as $[\text{Cs}^+]_2[\text{Na}^+][\text{As}_7]^{3-}$. Electronic band structure calculations confirm this reasoning.

Table 2. Selected bond distances (Å) and bond angles (°) in Cs_2NaAs_7 .

Atom pair	Distance	Angle label	Angle
As2–As1	2.4042(18)	As1–As2–As4	100.76(6)
As2–As4	2.4237(17)	As1–As2–As7	102.56(6)
As2–As7	2.4050(18)	As4–As2–As7	101.38(6)
As1–As3	2.348(2)	As2–As1–As3	98.97(6)
As4–As5	2.3411(18)	As2–As4–As5	98.90(6)
As7–As6	2.3465(19)	As2–As7–As6	98.45(6)
As3–As5	2.5139(19)	As3–As5–As6	59.98(5)
As3–As6	2.4964(19)	As5–As6–As3	60.68(5)
As5–As6	2.4799(17)	As6–As3–As5	59.33(5)

Figure 3. Representations of the $[\text{As}_7]^{3-}$ clusters in Cs_2NaAs_7 (a), $[\text{Zn}(1)\text{As}_{14}]^{4-}$ clusters in $\text{Cs}_4\text{ZnAs}_{14}$ (b), and the $[\text{CdAs}_{14}]^{4-}$ clusters in $\text{Cs}_4\text{CdAs}_{14}$ (c) with thermal ellipsoids, all drawn at the 50% probability level.



$\text{Cs}_4\text{ZnAs}_{14}$ crystallizes with an unusually large unit cell for an intermetallic compound ($V = 10309.9(14) \text{ \AA}^3$) and the structure is devoid of any disorder. The structure contains four crystallographically independent $[\text{ZnAs}_{14}]^{4-}$ polyanions, which are made up of tetrahedral Zn atoms, bridging two $[\text{As}_7]^{3-}$ clusters (Figure 3(b)). The structural complexity is apparently caused by the intricate orientation and packing of the $[\text{ZnAs}_{14}]^{4-}$ units. Interestingly, all the As atoms bonded to Zn are the 2-bonded As atoms at the waist of the $[\text{As}_7]^{3-}$ “birdcage”, wherein they could be assigned as negatively charged (the remaining As atoms are 3-bonded, and thus, with a formal charge 0). The same bonding features have also been revealed for the cluster compounds which have the similar structural motif, e.g., $[\text{K}(2,2,2\text{-crypt})]_3[\text{In}(\text{P}_7)_2] \cdot 3.5\text{py}$ [21], $[\text{K}(2,2,2\text{-crypt})]_4\text{ZnE}_{14}$ ($E = \text{P}, \text{As}$) [22], and $[\text{K}(2,2,2\text{-crypt})]_4\text{CdP}_{14} \cdot 6\text{py}$ [22]. The Zn–As bond distances fall in the range 2.514 to 2.598 Å, comparing well with the sum of their covalent radii [23], as well as with the corresponding distances found in other Zintl compounds with Zn–As bonding such as Ba_2ZnAs_2 [24], $\text{Eu}_{11}\text{Zn}_6\text{As}_{12}$ [25], and RbZn_4As_3 [26].

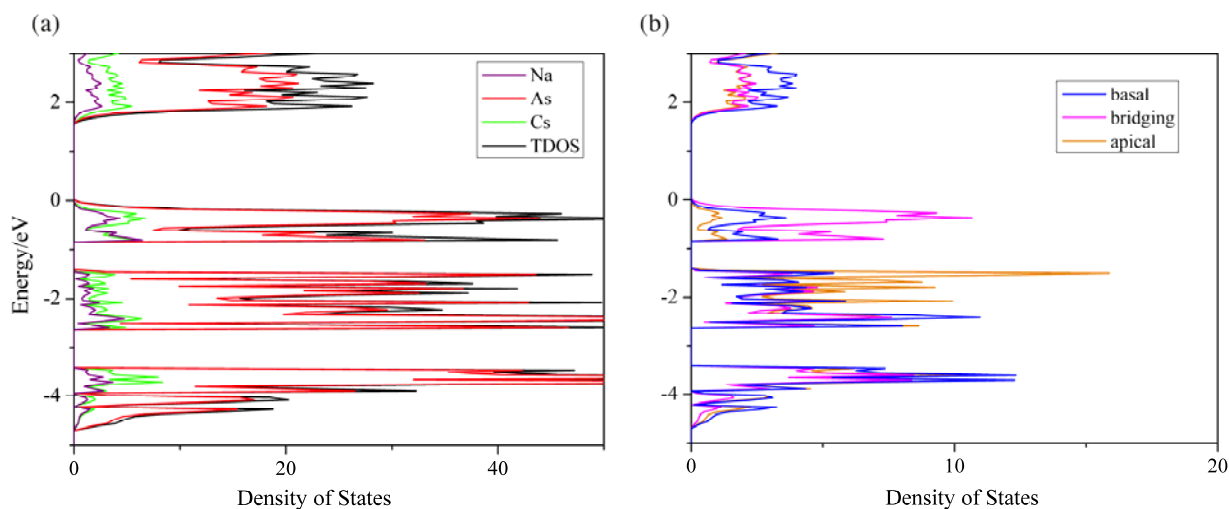
Table 3. Selected bond distances (Å) in $\text{Cs}_4\text{ZnAs}_{14}$ and $\text{Cs}_4\text{CdAs}_{14}$.

Atom pair	Distance	Atom pair	Distance
$\text{Cs}_4\text{ZnAs}_{14}$		$\text{Cs}_4\text{CdAs}_{14}$	
Zn1-tetrahedron		Cd-tetrahedron	
Zn1–As4	2.534(2)	Cd–As2	2.7364(10)
Zn1–As12	2.590(2)	Cd–As6	2.7736(10)
Zn1–As20	2.560(2)	Cd–As1	2.6957(9)
Zn1–As24	2.560(2)	Cd–As14	2.8241(11)
“birdcage” 1		“birdcage” 1	
As5–As4	2.441(2)	As3–As2	2.4339(11)
As5–As8	2.379(2)	As3–As6	2.4281(11)
As5–As12	2.425(2)	As3–As7	2.3741(11)
As4–As1	2.381(2)	As2–As8	2.3801(11)
As8–As7	2.363(3)	As6–As11	2.3775(12)
As12–As9	2.373(2)	As7–As12	2.3547(11)
As1–As7	2.479(2)	As8–As11	2.5025(11)
As1–As9	2.498(2)	As8–As12	2.5021(11)
As7–As9	2.463(2)	As11–As12	2.4545(12)
“birdcage” 2		“birdcage” 2	
As29–As20	2.4395(19)	As5–As1	2.4236(10)
As29–As24	2.425(2)	As5–As10	2.3873(11)
As29–As54	2.365(2)	As5–As14	2.4332(11)
As20–As16	2.368(2)	As1–As4	2.3951(11)
As24–As22	2.386(2)	As10–As13	2.3656(12)
As54–As26	2.361(2)	As14–As9	2.3760(11)
As16–As22	2.503(2)	As4–As13	2.4721(12)
As16–As26	2.489(2)	As4–As9	2.5090(11)
As22–As26	2.453(2)	As13–As9	2.4694(11)

Another interesting observation is the geometric distortion of the $[\text{As}_7]^{3-}$ moiety of the $[\text{ZnAs}_{14}]^{4-}$ anion compared to the isolated $[\text{As}_7]^{3-}$. Although the nortricyclane-like topology essentially remains intact, the “bidentate” coordination of the $[\text{As}_7]^{3-}$ ligand to the Zn atom induces some changes. For example, with a reference to the $[\text{Zn}(1)\text{As}_{14}]^{4-}$ species, the α angles involving the chelating As atoms significantly decrease ($\angle\text{As4-As5-As12} = 94.256^\circ$ and $\angle\text{As20-As29-As24} = 94.193^\circ$), concomitant with the slight increase of the bond distances (0.02–0.04 Å). On the other hand, the distances between the apical As and the bridging As atoms that are not bonded to Zn decrease ($\text{As5-As8} = 2.379$ Å, $\text{As29-As54} = 2.365$ Å) to a degree that they fall in the range of distances for the shortest set C (Table 3). Similar distortion is observed for all the eight $[\text{As}_7]^{3-}$ subunits, which again, are not symmetry-equivalent to each other. Examples in which the insertion of transition metals leads to more significant changes to the $[\text{Pn}_7]^{3-}$ cluster are also known from the organometallic literature. For instance, in the $[\text{E}_7\text{M}(\text{CO})_3]^{3-}$ clusters ($E = \text{P, As, Sb}$ and $M = \text{Cr, Mo, W}$) [27,28], the nortricyclane-like E_7^{3-} fragments transformed into norbornadiene-like clusters due to the four bonds between the transition metal and two of the bridging and two of the basal pnictogens. More profound change has been noted in $[\text{Sb}_7\text{Ni}_3(\text{CO})_3]^{3-}$ [29], where the Sb_7^{3-} is bonded to three Ni atoms, forming a 10-vertex *nido* cluster.

$\text{Cs}_4\text{CdAs}_{14}$ crystallizes with the same space group as $\text{Cs}_4\text{ZnAs}_{14}$, however, with only one $[\text{CdAs}_{14}]^{4-}$ polyanion in the asymmetric unit. The Cd atoms are tetrahedrally bonded to the As atoms from two adjacent $[\text{As}_7]^{3-}$ clusters, with average Cd–As distance of 2.757 Å, which is just slightly larger than the sum of their covalent radii ($r_{\text{Cd}} = 1.38$ Å; $r_{\text{As}} = 1.21$ Å) [23]. In both $\text{Cs}_4\text{ZnAs}_{14}$ and $\text{Cs}_4\text{CdAs}_{14}$, the $[\text{ZnAs}_{14}]^{4-}$ and $[\text{CdAs}_{14}]^{4-}$ anions form a simple cubic array (very distorted in the case of $\text{Cs}_4\text{ZnAs}_{14}$). Compared with the ZnAs_4 tetrahedra in the analogous $[\text{ZnAs}_{14}]^{4-}$ motif of $\text{Cs}_4\text{ZnAs}_{14}$, the CdAs_4 tetrahedra are more distorted. This can be seen from an inspection of the As–Cd–As angles, which deviate more from the ideal 109.5° tetrahedral angle. The $[\text{As}_7]^{3-}$ units experience similar geometric distortion due to the “bidentate” coordination to Cd; however, comparison of the corresponding distances (Table 3) and angles reveals that the distortion in $[\text{CdAs}_{14}]^{4-}$ is less pronounced. This is understandable since the longer Cd–As distances would naturally allow more flexibility.

Figure 4. (a) Total and partial density of states (DOS) for Cs_2NaAs_7 . (b) Comparison of the average DOS of the different As atoms (see text for details).



Following the above discussion, the electron count in both $\text{Cs}_4\text{ZnAs}_{14}$ and $\text{Cs}_4\text{CdAs}_{14}$ could be assigned in the same way: $(\text{Cs}^+)_4(4b\text{-Zn}^{2-})(3b\text{-As}^0)_{12}(2b\text{-As}^-)_2$ and $(\text{Cs}^+)_4(4b\text{-Cd}^{2-})(3b\text{-As}^0)_{12}(2b\text{-As}^-)_2$, which is in consistent with the Zintl formalism [2]. Exaggerating the ionicity of the Zn–As and Cd–As interactions, the formula units can also be broken down as $[\text{Cs}^+]_4[\text{Zn}^{2+}]\{[\text{As}_7]^{3-}\}_2$ and $[\text{Cs}^+]_4[\text{Cd}^{2+}]\{[\text{As}_7]^{3-}\}_2$, respectively.

The electronic structure of Cs_2NaAs_7 was calculated using the LMTO method [14–16] and the plot of the total and partial density of states is shown in Figure 4(a). A band-gap in the order of 1.6 eV is noticeable from the plot, suggesting that Cs_2NaAs_7 should be an intrinsic semiconductor. Note that the LMTO method usually underestimates the band-gap, this value actually agrees very well with the dark red color of the crystals. Due to the low symmetry and very complex structures of $\text{Cs}_4\text{ZnAs}_{14}$ and $\text{Cs}_4\text{CdAs}_{14}$, the electronic structures for neither were carried out; the appearance of their crystals also suggested semiconducting behavior with a band-gap in the visible range.

Analyzing the electronic structure of Cs_2NaAs_7 , one can readily see that the states below the Fermi level in the range from -5 to 0 eV (set as the Fermi level) are predominately contributed from As p orbitals, with only a small admixture of states from the alkali metals, in agreement with the Zintl formalism. In the vicinity of the Fermi level, however, the contributions of the three different types of As atoms differ very much, as seen from Figure 4(b). The apical As atom has almost negligible partial DOS, while the contribution from the As atoms at the bridging position (waist of the cluster) is significant in this energy window. Such characteristics of the electronic structure should indicate different chemical and physical properties of As atoms at different positions, *i.e.*, chemical reactivity.

3. Experimental Section

All manipulations involving the alkali metals were performed either inside an argon-filled glove box with controlled moisture/oxygen levels or under vacuum. Crystals of Cs_2NaAs_7 , $\text{Cs}_4\text{ZnAs}_{14}$, and $\text{Cs}_4\text{CdAs}_{14}$ were all identified from reactions originally aimed at the pnictide clathrates $\text{Cs}_8\text{Zn}_{18}\text{As}_{28}$, $\text{Cs}_8\text{Cd}_{18}\text{As}_{28}$ or the mixed-cation variant $\text{Na}_6\text{Cs}_2\text{Zn}_{18}\text{As}_{28}$. In the typical reactions, the elements (Na/Cs/Ca/Zn/Cd/As, purchased from either Alfa Aesar or Aldrich with the stated purity higher than 99.9%, used as received) with the desired stoichiometric ratio were loaded into niobium ampoules. The niobium ampoules were arc-welded under high purity Ar and then jacketed within fused silica tubes, which were subsequently flame-sealed under vacuum. The reaction mixtures were heated up to 500 °C in a programmable furnace, and equilibrated for 1 week before being slowly cooled to room temperature. The dark red crystals of Cs_2NaAs_7 were initially identified as a byproduct of a reaction with starting elements Na, Cs, Zn, and As, carried out as described above. The major product was CsZn_4As_3 [26], with Zn_3As_2 [30] and Cs_2NaAs_7 as side products. Cs_2NaAs_7 can be made as phase pure material from stoichiometric mixture without Zn.

From an analogous reaction with starting elements Na, Cs, Cd, and As, $\text{Cs}_4\text{CdAs}_{14}$ was initially identified, together with $\text{Cs}_8\text{Cd}_{18}\text{As}_{28}$ [31], NaCd_4As_3 [26], and CdAs_2 [32]. The differentiation from the other phases was possible due to the red color and transparent habit of the crystals. $\text{Cs}_4\text{ZnAs}_{14}$ was originally obtained from a reaction loaded as $\text{Ca}_{16}\text{Cs}_8\text{Zn}_{58.67}\text{As}_{77.33}$, and subjected to the above-described heat treatment. The dark red crystals in this reaction were identified as $\text{Cs}_4\text{ZnAs}_{14}$, between the black crystals of CaZn_2As_2 [33] and the silvery ones of Zn_3As_2 [30]. After the structures and the

compositions were established from single-crystal diffraction work, $\text{Cs}_4\text{CdAs}_{14}$ and $\text{Cs}_4\text{ZnAs}_{14}$ were synthesized in high yield from the corresponding stoichiometric reactions.

All three compounds degraded quickly upon exposure to air.

The crystal structures of the title compounds were established using single-crystal X-ray diffraction. The diffraction data were collected on a Bruker SMART CCD-based diffractometer using monochromated $\text{Mo K}\alpha_1$ radiation. Crystals were cut to suitable dimensions ($<100\ \mu\text{m}$) under a microscope and then mounted on glass fiber with Paratone-N oil. The fiber was then quickly transferred to the goniometer of the diffractometer, where a cold nitrogen stream (200(2) K) was used to harden the oil in order to protect the crystals from being oxidized. Full spheres of data were collected in four batch runs with a frame width of 0.3° for ω and θ . Integration of the intensity data was done with SAINT program [34], and semi-empirical absorption correction based on equivalents was applied with the SADABS code [35]. The structures were solved by direct method and refined to convergence by full matrix least squares on F^2 using the SHELXTL package [36]. The atomic coordinates were standardized with the aid of the Structure TIDY [37]. In the last refinement cycles, all atoms were treated with anisotropic displacement parameters. Tables with selected refinement parameters and the atomic coordinates and equivalent isotropic displacement parameters are submitted as electronic supplementary information. Selected crystal data and refinement parameters are given in Table 1; important bond distances and angles are listed in Table 2 and Table 3. CIFs have also been deposited with Fachinformationszentrum Karlsruhe, 76344 Eggenstein-Leopoldshafen, Germany, (fax: (49) 7247-808-666; e-mail: crysdata@fiz.karlsruhe.de)—depository numbers CSD-423080 for Cs_4NaAs_7 , CSD-423081 for $\text{Cs}_4\text{CdAs}_{14}$, and CSD-423082 for $\text{Cs}_4\text{ZnAs}_{14}$.

The Stuttgart TB-LMTO 4.7 code [38], which employs the tight-binding linear muffin-tin orbital (TB-LMTO) method [14-16], was used to calculate the band structures of Cs_2NaAs_7 . In this program, local density approximation (LDA) was used to treat exchange and correlation [39]. All relativistic effects except for spin-orbital coupling were taken into account by scalar relativistic approximation [40]. Due to the limited computing resources, $\text{Cs}_4\text{CdAs}_{14}$ and $\text{Cs}_4\text{ZnAs}_{14}$ (very complex and large structures) could not be treated. For the calculation of Cs_2NaAs_7 , the basis set included the $6s$, $6p$, $5d$ and $4f$ orbitals for Cs, $3s$, $3p$ and $3d$ orbitals for Na, and $4s$, $4p$ and $4d$ orbitals for As. The $6p$, $5d$ and $4f$ orbitals of Cs, $3p$ and $3d$ orbitals of Na, and $4d$ orbital of As were treated with the downfolding technique [41]. The total and partial density of states were plotted with the Fermi level set as a reference at 0 eV.

4. Conclusions

Three new Zintl phases Cs_2NaAs_7 , $\text{Cs}_4\text{ZnAs}_{14}$ and $\text{Cs}_4\text{CdAs}_{14}$ have been synthesized via high temperature reactions. The structure of Cs_2NaAs_7 features the nortricyclane-like cluster $[\text{As}_7]^{3-}$, while the structures of the latter two contain very large $[\text{ZnAs}_{14}]^{4-}$ and $[\text{CdAs}_{14}]^{4-}$ anions, which are composed of two $[\text{As}_7]^{3-}$ units, linked by 4-coordinated Zn or Cd. Band structure calculations confirm the intrinsic semiconductor with a size of band-gap consistent with the dark red color of the crystals.

Supplementary Material

Supplementary data associated with this article can be found in the online version at doi: 10.3390/cryst1030087.

Acknowledgments

Svilen Bobev acknowledges financial support from the US Department of Energy through a grant (DE-SC0001360).

References

1. Zintl, E. Intermetallische Verbindungen. *Angew. Chem.* **1939**, *52*, 1-6.
2. Schäfer, H.; Eisenman, B.; Müller, W. Zintl Phases-Transitions between Metallic and Ionic Bonding. *Angew. Chem. Int. Ed.* **1973**, *12*, 694-712.
3. Kauzlarich, S.M.; Brown, S.R.; Snyder, G.J. Zintl Phases for Thermoelectric Devices. *Dalton Trans.* **2007**, 2099-2107.
4. Brown, S.R.; Kauzlarich, S.M.; Gascoin, F.; Snyder, G.J. Yb₁₄MnSb₁₁: New High Efficiency Thermoelectric Material for Power Generation. *Chem. Mater.* **2006**, *18*, 1873-1877.
5. Gascoin, F.; Ottensmann, S.; Stark, D.; Haile, S.M.; Snyder, G.J. Zintl Phases as Thermoelectric Materials: Tuned Transport Properties of the Compounds Ca_xYb_{1-x}Zn₂Sb₂. *Adv. Funct. Mater.* **2005**, *15*, 1860-1864.
6. Zhang, H.; Zhao, J.-T.; Grin, Y.; Wang, X.-J.; Tang, M.-B.; Man, Z.-Y.; Chen, H.-H.; Yang, X.-X. A New Type of Thermoelectric Material, EuZn₂Sb₂. *J. Chem. Phys.* **2008**, *129*, 164713.
7. Kolis, J.W.; Young, D.M. Molecular Transition Metal Complexes of Zintl Ions. In *Chemistry, Structure, and Bonding of Zintl Phases and Ions*; Kauzlarich, S.M., Ed.; VCH: New York, NY, USA, 1996; pp. 225-244.
8. Corbett, J.D. Polyatomic Zintl Anions of the Post-Transition Elements. *Chem. Rev.* **1985**, *85*, 383-397.
9. Sun, D.; Riley, A.E.; Cadby, A.J.; Richman, E.K.; Korlann, S.D.; Tolbert, S.H. Hexagonal Nanoporous Germanium through Surfactant-Driven Self-Assembly of Zintl Clusters. *Nature* **2006**, *441*, 1126-1130.
10. Korlann, S.D.; Riley, A.E.; Mun, B.S.; Tolbert, S.H. Chemical Tuning of the Electronic Properties of Nanostructured Semiconductor Films Formed through Surfactant Templating of Zintl Cluster. *J. Phys. Chem. C* **2009**, *113*, 7697-7705.
11. Moses, M.J.; Fettinger, J.C.; Eichhorn, B.W. Interpenetrating As₂₀ Fullerene and Ni₁₂ Icosahedra in the Onion-Skin [As@Ni₁₂@As₂₀]³⁻ Ion. *Science* **2003**, *300*, 778-780.
12. Esenturk, E.N.; Fettinger, J.C.; Eichhorn, B.W. The Pb₁₂²⁻ and Pb₁₀²⁻ Zintl Ions and the M@Pb₁₂²⁻ and M@Pb₁₀²⁻ Cluster Series Where M = Ni, Pd, Pt. *J. Am. Chem. Soc.* **2006**, *128*, 9178-9186.
13. Hull, M.W.; Sevov, S.C. Functionalization of Nine-Atom Deltahedral Zintl Ions with Organic Substituents: Detailed Studies of the Reactions. *J. Am. Chem. Soc.* **2009**, *131*, 9026-9037.
14. Andersen, O.K. Linear Methods in Band Theory. *Phys. Rev. B* **1975**, *12*, 3060-3083.

15. Andersen, O.K.; Jepsen, O. Explicit, First-Principles Tight-Binding Theory. *Phys. Rev. Lett.* **1984**, *53*, 2571-2574.
16. Andersen, O.K.; Pawłowska, Z.; Jepsen, O. Illustration of the Linear Muffin-Tin Orbital Tight-Binding Representation: Compact Orbitals and Charge Density in Si. *Phys. Rev. B* **1986**, *34*, 5253-5269.
17. Hönle, W.; Buresch, J.; Peters, K.; Chang, J.-H.; von Schnering, H.G. Crystal structure of the low-temperature modification of trilithium heptaarsenide, LT-Li₃As₇. *Z. Kristallogr.* **2002**, *217*, 485-486.
18. Hönle, W.; Buresch, J.; Peters, K.; Chang, J.-H.; von Schnering, H.G. Crystal structure of the low-temperature modification of trisodium heptaarsenide, LT-Na₃As₇. *Z. Kristallogr.* **2002**, *217*, 487-488.
19. Emmerling, F.; Röhr, C. Alkali Metal Arsenides A₃As₇ and AAs (A = K, Rb, Cs). Preparation, Crystal Structure, Vibrational Spectroscopy. *Z. Naturforsch.* **2002**, *57b*, 963-975.
20. Hanauer, T.; Grothe, M.; Reil, M.; Korber, N. Syntheses and Crystal Structures of Four New Ammoniates with Heptaarsenide (As₇³⁻) Anions. *Helv. Chim. Acta* **2005**, *88*, 950-961.
21. Knapp, C.M.; Large, J.S.; Rees, N.H.; Goicoechea, J.M. A Versatile Salt-Metathesis Route to Heteroatomic Clusters Derived from Phosphorus and Arsenic Zintl Anions. *Dalton Trans.* **2011**, *40*, 735-745.
22. Knapp, C.M.; Zhou, B.; Denning, M.S.; Rees, N.H.; Goicoechea, J.M. Reactivity Studies of Group 15 Zintl Ions towards Homoleptic Post-Transition Metal Organometallics: a 'Bottom-up' Approach to Bimetallic Molecular. *Dalton Trans.* **2010**, *39*, 426-436.
23. Pauling, L. *The Nature of the Chemical Bond*, 3rd ed.; Cornell University Press: Ithaca, NY, USA, 1960; pp. 400-404.
24. Saparov, B.; Bobev, S. Isolated $_{\infty}^1[\text{ZnPn}_2]^{4-}$ Chains in the Zintl Phases Ba₂ZnPn₂ (Pn = As, Sb, Bi) – Synthesis, Structure, and Bonding. *Inorg. Chem.* **2010**, *49*, 5173-5179.
25. Saparov, B.; Bobev, S. Undecaeuropium hexazinc dodecaarsenide. *Acta Crystallogr.* **2010**, *E66*, i24.
26. He, H.; Tyson, C.; Bobev, S. 8-coordinated Arsenic in the Zintl Phases RbCd₄As₃ and RbZn₄As₃. Synthesis and Structural Characterization. *Inorg. Chem.* **2011**, submitted for publication.
27. Eichhorn, B.W.; Haushalter, R.C.; Huffman, J.C. Insertion of Cr(CO)₃ into As₇³⁻ to Form [As₇Cr(CO)₃]³⁻: An Inorganic Nortricyclane-to-Norbornadiene Conversion. *Angew. Chem. Int. Ed.* **1989**, *28*, 1032-1033.
28. Charles, S.; Eichhorn, B.W.; Rheingold, A.L.; Bott, S.G. Synthesis, Structure, and Properties of the [E₇M(CO)₃]³⁻ Complexes Where E = P, As, Sb and M = Cr, Mo, W. *J. Am. Chem. Soc.* **1994**, *116*, 8077-8086.
29. Charles, S.; Eichhorn, B.W.; Bott, S.G. Synthesis and Structure of [Sb₇Ni₃(CO)₃]³⁻: A New Structural Type for *nido* 10-Vertex Polyhedral Clusters. *J. Am. Chem. Soc.* **1993**, *115*, 5837-5838.
30. Wegłowski, S.; Lukaszewicz, K. The Crystal Structure of Zinc Arsenide polymorphic modifications α-Zn₃As₂ and α'-Zn₃As₂. *Bull. Acad. Polon. Sci. Ser. Sci. Chim.* **1968**, *16*, 177-182.
31. He, H.; Bobev, S. type-I clathrate Cs₈Cd₁₈As₂₈, space group $Pm\bar{3}n$, *a* = 11.3281(5) Å. Unpublished results, 2011.

32. Cervinka, L.; Hruby, A. The Crystal Structure of CdAs₂. *Acta Crystallogr.* **1970**, *26B*, 457-458.
33. Klüfers, P.; Mewis, A. AB₂X₂ – Verbindungen im CaAl₂Si₂-typ. III. Zur Struktur der Verbindungen CaZn₂P₂, CaCd₂P₂, CaZn₂As₂, und CaCd₂As₂. *Z. Naturforsch.* **1977**, *32b*, 753-756.
34. *SAINTE*, Version 6.45; Bruker Analytical X-ray Systems, Inc.: Madison, WI, USA, 2003.
35. Sheldrick, G.M. *SADABS*; University of Göttingen: Göttingen, Germany, 2003.
36. Sheldrick, G.M. *SHELXTL*; University of Göttingen: Göttingen, Germany, 2001.
37. Gelato, L.M., Parthe, E. Structure Tidy - a Computer Program to Standardize Crystal Structure Data. *J. Appl. Crystallogr.* **1987**, *20*, 139-146.
38. Jepsen, O.; Andersen, O.K. *TB-LMTO-ASA Program*, version 4.7; Max-Planck-Institut für Festkörperforschung: Stuttgart, Germany, 1998.
39. von Barth, U.; Hedin, L. Local Exchange-Correlation Potential for Spin Polarized Case 1. *J. Phys. C: Solid State Phys.* **1972**, *5*, 1629-1642.
40. Koelling, D.D.; Harmon, B.N. Technique for Relativistic Spin-Polarized Calculations. *J. Phys. C Solid State Phys.* **1977**, *10*, 3107-3114.
41. Lambrecht, W.R.L.; Andersen, O.K. Minimal Basis-Sets in the Linear Muffin-Tin Orbital Method – Application to the Diamond-Structure Crystals C, Si, and Ge. *Phys. Rev. B: Condens. Matter* **1986**, *34*, 2439-2449.

© 2011 by the authors; licensee MDPI, Basel, Switzerland. This article is an open access article distributed under the terms and conditions of the Creative Commons Attribution license (<http://creativecommons.org/licenses/by/3.0/>).